Aalborg Universitet

AALBORG UNIVERSITY

DENMARK

Tracking of the Multi-Dimensional Parameters of a Target Signal using Particle Filtering

Yin, Xuefeng; Pedersen, Troels; Steinböck, Gerhard; Kirkelund, Gunvor; Blattnig, Peter; Jaquier, Alain; Fleury, Bernard Henri

Tracking of the Multi-Dimensional Parameters of a Target Signal using Particle Filtering

Xuefeng Yin[1], Troels Pedersen[1], Gerhard Steinböck[1], Gunvor Elisabeth Kirkelund[1],
Peter Blattnig[2], Alain Jaquier[2], and Bernard H. Fleury[1,3]
[1]Section Navigation and Communications, Department of Electronic Systems,
Aalborg University, DK-9220, Aalborg, Denmark
[2] Federal Department for Defence, Civil Protection and Sports, armasuisse, Science and Technology, Switzerland
[3]Forschungszentrum Telekommunikation Wien (ftw.), Vienna, Austria
Email: xuefeng@es.aau.dk

Abstract— In this contribution, a low-complexity particle filter (PF) is proposed to track the parameters of the signal reflected by a target illuminated with a digital-video-broadcast terrestrial (DVB-T) signal. The tracked parameters are the delay (time of arrival), the azimuth and elevation of arrival, the Doppler frequency, the complex amplitude of the target signal, as well as the rates of change of all but the last parameter. The proposed PF tracks these parameters based on samples of the target signal by assuming that the temporal behaviour of these parameters is governed by a multi-dimensional linear state-space model. The algorithm has an additional resampling step specifically designed to cope with the highly concentrated multi-dimensional posterior probability density function of the parameters. This step allows for tracking the parameters of the target signal with only a few particles, e.g. 50, leading to low computational complexity. Simulation results show that the PF outperforms the maximum-likelihood estimator applied to individual samples of the target signal in terms of higher accuracy and robustness. Under certain conditions usually met in reality the proposed PF can be used to track the parameters of the signals contributed by individual targets in multi-target scenarios.

Index Terms— Target tracking, bistatic passive radar, antenna array, maximum likelihood estimation, terrestrial digital-video-broadcasting, and particle filter.

I. Introduction

Target tracking algorithms can be grouped into two categories: the conventional algorithms [1], [2], [3], [4] and the track-before-detection (TBD) algorithms proposed recently [5], [6], [7], [8]. The conventional algorithms operate in three successive stages [3], [4], [8], which are *i)* estimation of the parameters, such as delay (time of arrival), Doppler frequency and angle of arrival, of the signals reflected by targets, and detection of the target signals using thresholding techniques [4], *ii)* association of the parameter estimates to individual tracks, one for each target, and *iii)* estimation of the target trajectories in a Cartesian coordinate system from these tracks. In some conventional algorithms, e.g. the particle-filter-based method proposed in [2], [3], the latter two stages are performed jointly as one single stage. The TBD algorithms exhibit two stages [5], [6], [7], i.e. *i)* estimation of the dispersion power spectrum from each sample of the received signal, and *ii)* estimation of the target trajectories from the power spectrum estimates. Since the TBD algorithms do not implement any

detection operation based on thresholding, they are capable of tracking weak targets that are undetected with the conventional approaches. Following the nomenclature used in [9] we refer to the (complex baseband) signal reflected by a target at the output of the radar receiver as the "target signal" in the sequel.

The tracking algorithms in the above two categories share the common feature that the basis for extraction of target position trajectories, i.e. the estimates of the target signal parameters in the conventional algorithms and the estimates of the dispersion power spectrum in the TBD algorithms, are all computed *independently* from individual observations of the received signal. Thus these algorithms do not consider the behaviour of the temporal evolution of the parameters of the target signals. As we will see, exploiting this information leads to a significant performance increase in terms of estimation accuracy and robustness.

In this contribution, we propose a particle filter (PF) for tracking of the multi-dimensional parameters of the signal induced by one target. The temporal evolution of the parameters is characterized using a linear state-space model. We implement the PF in a passive bistatic radar system which uses a digital-video-broadcasting terrestrial (DVB-T) signal as "illuminator of opportunity". The receiver is equipped with multiple antennas which are activated in a time-division-multiplexing (TDM) mode. Simulations are performed in a single-target scenario for evaluation of the performance of the proposed PF.

The organization of the paper is as follows. Section II presents an observation model of the target signal and a state-space model characterizing the time-evolution behaviour of the parameters of the observation model. In Section III, the proposed PF is formulated. Section IV describes the results of simulation studies that illustrate the performance of the PF. Concluding remarks are addressed in Section V.

II. Signal Model

In this section, an observation model for the target signal is introduced. Then, a state-space model is used to describe the time-evolving behaviour of the signal parameters. For simplicity of the presentation, these models are discussed while considering a single-target scenario with one DVB-T transmitter (Tx) and one radar receiver (Rx) and the received signal is assumed to contain only the target signal and noise.
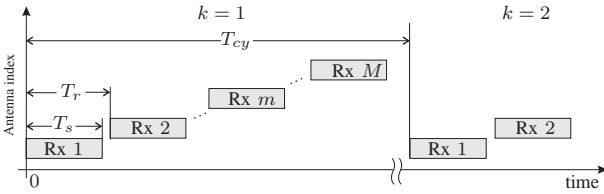
Fig. 1. A TDM switching mode used in the radar receiver.

A. Observation Model

In the considered bistatic radar, the Rx is equipped with M antennas. A switch is used to activate these antennas in a predefined TDM mode. Compared to parallel schemes where all receive antennas are activated simultaneously, this switching structure can reduce the hardware cost and the complexity of the equipment calibration. An example of TDM mode is depicted in Fig. 1. In this mode, the Rx antennas are activated sequentially from No. 1 to M in one measurement cycle. A measurement cycle is referred to as the procedure in which all receive antennas are scanned once. In Fig. 1, k and m represent respectively the measurement cycle index and the antenna index, T_s denotes the sensing period during which an antenna is activated, the switching period T_r is referred to as the time interval between consecutive sensing periods, and the cycle period T_{cy} denotes the interval between two consecutive measurement cycles.

In the kth measurement cycle, the complex baseband signal received in the sensing period for the mth Rx antenna reads

$$y_{k,m}(t) = x(t; \boldsymbol{\theta}_{k,m}) + n_{k,m}(t), \quad t \in [t_{k,m}, t_{k,m} + T_s), \quad (1)$$

where $t_{k,m}$ denotes the beginning of this sensing period, and the parameter vector

$$\boldsymbol{\theta}_{k,m} \doteq [\alpha_{k,m}, \nu_{k,m}, \phi_{k,m}, \theta_{k,m}, \tau_{k,m}]$$

contains the complex gain $\alpha_{k,m}$, Doppler frequency $\nu_{k,m}$, azimuth $\phi_{k,m}$ and elevation $\theta_{k,m}$ of arrival, and delay $\tau_{k,m}$ of the target signal in this sensing period.

The signal contribution $x(t; \boldsymbol{\theta}_{k,m})$ in (1) is written as

$$x(t; \boldsymbol{\theta}_{k,m}) = \alpha_{k,m} \exp(j2\pi\nu_{k,m}t) \cdot c_m(\phi_{k,m}, \theta_{k,m})$$
$$\cdot u(t - \tau_{k,m}), \quad t \in [t_{k,m}, t_{k,m} + T_s), \quad (2)$$

where $c_m(\phi, \theta)$ represents the response of the mth antenna in the direction uniquely determined by azimuth ϕ and elevation θ, while $u(t - \tau)$ denotes the DVB-T signal delayed by τ. In this contribution, we assume that $u(t)$ is known. This is a realistic assumption, as in most passive radar systems the transmitted signal can be obtained by using a reference antenna which receives the signals directly from the Tx [1], [10]. The noise $n_{k,m}(t)$ in (1) is a zero-mean Gaussian process with spectrum height σ_n^2. For notational convenience, we use the vector $\boldsymbol{y}_k$ to represent all samples received within the kth measurement cycle and $\boldsymbol{y}_{1:k} \doteq \{\boldsymbol{y}_1, \boldsymbol{y}_2, \ldots, \boldsymbol{y}_k\}$ to denote the observations up to the kth cycle.

We consider the scenario where the Rx switch operates fast enough, such that the approximation $\boldsymbol{\theta}_{k,m} \approx \boldsymbol{\theta}_k$ holds for $m = 1, \ldots, M$. Then, the target signal $x(t; \boldsymbol{\theta}_{k,m})$ in (2) is approximated by

$$x(t; \boldsymbol{\theta}_k) = \alpha_k \exp(j2\pi\nu_k t) \cdot c_m(\phi_k, \theta_k)$$
$$\cdot u(t - \tau_k), \quad t \in [t_{k,m}, t_{k,m} + T_s). \quad (3)$$

From (3), we see that in the kth measurement cycle, the transmitted signal is modulated at the receiver by a phasor depending on the Doppler frequency ν_k. Thus, it is possible to use the signals received in one measurement cycle to estimate the Doppler frequency.

B. State-Space Model

We use a state-space model to describe the transition of the signal parameters across measurement cycles. We define the state vector in the kth measurement cycle as

$$\boldsymbol{\Omega}_k \doteq \begin{bmatrix} \boldsymbol{\varphi}_k \\ \boldsymbol{\alpha}_k \\ \boldsymbol{\Delta}_k \end{bmatrix}, \quad (4)$$

where the vectors

$$\boldsymbol{\varphi}_k \doteq \begin{bmatrix} \tau_k \\ \phi_k \\ \theta_k \\ \nu_k \end{bmatrix}, \boldsymbol{\Delta}_k \doteq \begin{bmatrix} \Delta\tau_k \\ \Delta\phi_k \\ \Delta\theta_k \\ \Delta\nu_k \end{bmatrix} \text{ and } \boldsymbol{\alpha}_k \doteq \begin{bmatrix} |\alpha_k| \\ \arg(\alpha_k) \end{bmatrix} \quad (5)$$

represent respectively the "dispersion parameter" vector, the "rates of change" vector, and the "(complex) gain" vector. In (5), $|\alpha_k|$ and $\arg(\alpha_k)$ represent the magnitude and the argument of α_k respectively.

The state vector at the kth cycle is modelled as

$$\underbrace{\begin{bmatrix} \boldsymbol{\varphi}_k \\ \boldsymbol{\alpha}_k \\ \boldsymbol{\Delta}_k \end{bmatrix}}_{\boldsymbol{\Omega}_k} = \underbrace{\begin{bmatrix} \boldsymbol{I}_4 & \boldsymbol{0}_{4\times2} & T_{cy}\boldsymbol{I}_4 \\ \boldsymbol{J}_k & \boldsymbol{I}_2 & \boldsymbol{0}_{2\times4} \\ \boldsymbol{0}_{4\times4} & \boldsymbol{0}_{4\times2} & \boldsymbol{I}_4 \end{bmatrix}}_{\boldsymbol{F}_k} \underbrace{\begin{bmatrix} \boldsymbol{\varphi}_{k-1} \\ \boldsymbol{\alpha}_{k-1} \\ \boldsymbol{\Delta}_{k-1} \end{bmatrix}}_{\boldsymbol{\Omega}_{k-1}} + \underbrace{\begin{bmatrix} \boldsymbol{0}_{4\times1} \\ \boldsymbol{v}_{\boldsymbol{\alpha},k} \\ \boldsymbol{v}_{\boldsymbol{\Delta},k} \end{bmatrix}}_{\boldsymbol{v}_k}, \quad (6)$$

where $\boldsymbol{I}_n$ represents the $n \times n$ identity matrix, $\boldsymbol{0}_{b\times c}$ is the all-zero matrix of dimension $b \times c$, and the matrix $\boldsymbol{J}_k$ reads

$$\boldsymbol{J}_k = \begin{bmatrix} 0 & 0 & 0 & 0 \\ 0 & 0 & 0 & 2\pi T_{cy} \end{bmatrix}.$$

The vector $\boldsymbol{v}_k$ in (6) contains the driving process $\boldsymbol{v}_{\boldsymbol{\alpha},k}$ of the gain vector and the driving process $\boldsymbol{v}_{\boldsymbol{\Delta},k}$ of the rates of change vector, i.e.

$$\boldsymbol{v}_{\boldsymbol{\alpha},k} \doteq \begin{bmatrix} v_{|\alpha|,k} \\ v_{\arg(\alpha),k} \end{bmatrix} \text{ and } \boldsymbol{v}_{\boldsymbol{\Delta},k} \doteq \begin{bmatrix} v_{\Delta\tau,k} \\ v_{\Delta\phi,k} \\ v_{\Delta\theta,k} \\ v_{\Delta\nu,k} \end{bmatrix}. \quad (7)$$

The entries $v_{(\cdot),k}$ of $\boldsymbol{v}_{\boldsymbol{\alpha},k}$ and $\boldsymbol{v}_{\boldsymbol{\Delta},k}$ are independent zero-mean Gaussian random variables with known variances: $v_{(\cdot),k} \sim \mathcal{N}(0, \sigma_{(\cdot)}^2)$.

III. THE PARTICLE FILTER

From (1) and (6), we see that the received signal $\boldsymbol{y}_k$ depends only on the current state $\boldsymbol{\Omega}_k$ and is conditionally independent of the other states given $\boldsymbol{\Omega}_k$. Utilizing this property, a PF can be used to estimate the posterior probability density function (pdf) $p(\boldsymbol{\Omega}_{1:k}|\boldsymbol{y}_{1:k})$ sequentially [11]. Here, $\boldsymbol{\Omega}_{1:k} \doteq \{\boldsymbol{\Omega}_1, \ldots, \boldsymbol{\Omega}_k\}$ denotes the sequence of state vectors from the 1st to the (k)th measurement cycle. The facts that the parameter space is multi-dimensional[1] and that the temporal

[1]The parameter space has dimension up to 14 in the specular-path scenario [12] and up to 28 in the dispersive-path scenario [13].

and spatial observation aperture has to be large in order to achieve high resolution pose a noticeable challenge when using the PF to track $\mathbf{\Omega}_k$. Indeed in this case, the posterior pdf $p(\mathbf{\Omega}_{1:k}|\mathbf{y}_{1:k})$ is highly concentrated in the multi-dimensional parameter space. It is then difficult to "steer" the particle sets to the regions where most of the posterior probability mass is localized. The proposed PF is specifically designed to solve this problem. In this section we present the PF while considering a single-target scenario. We also discuss the extension of the PF for tracking the parameters of the signals contributed by multiple targets.

A. Initialization of the Particle States

In this contribution, we use the proposed PF to track $\mathbf{\Omega}_k$ from the third measurement cycle on. The state for the ith particle at the second measurement cycle, denoted by $\mathbf{\Omega}_2^i$, is initialized with the parameter estimates obtained by using a sample-based maximum likelihood (ML) method. This method computes estimates of the parameters of the target signal from each individual sample gathered from the measurement cycles. Thus, the method assumes that the parameters of the target signal samples in different measurement cycles are independent. The dispersion parameter vector $\boldsymbol{\varphi}_2^i$ is set equal to its corresponding sample-based ML estimate computed from the signal sample collected at the second measurement cycle. The rate of change parameters are initialized by taking the difference between the sample-based ML estimates obtained in the first and second measurement cycles.

B. The Steps of the PF

When a new observation, say $\mathbf{y}_k$, is available, the PF performs the following steps.

Step 1: Predict the states of particles and calculate their importance weights. The output from the previous observations is the set $\{\mathbf{\Omega}_{k-1}^i, w_{k-1}^i\}$, where w_{k-1}^i denotes the importance weight of the ith particle. We first predict the states of all particles for the kth measurement cycle. The rates of change vector $\mathbf{\Delta}_k^i$ is updated as

$$\mathbf{\Delta}_k^i = \mathbf{\Delta}_{k-1}^i + \boldsymbol{v}_{\mathbf{\Delta},k}^i, \quad i = 1, \ldots, I, \tag{8}$$

where I denotes the total number of particles, and the vector $\boldsymbol{v}_{\mathbf{\Delta},k}^i$ is drawn from a $\mathcal{N}(\mathbf{0}, \mathbf{\Sigma}_{\boldsymbol{v}_{\mathbf{\Delta}}})$ distribution. The diagonal covariance matrix $\mathbf{\Sigma}_{\boldsymbol{v}_{\mathbf{\Delta}}}$ reads

$$\mathbf{\Sigma}_{\boldsymbol{v}_{\mathbf{\Delta}}} = \mathrm{diag}(\sigma_{\Delta\tau}^2, \sigma_{\Delta\phi}^2, \sigma_{\Delta\theta}^2, \sigma_{\Delta\nu}^2). \tag{9}$$

The values of the diagonal elements $\sigma_{\Delta(\cdot)}^2$ with $(\cdot)$ replaced by τ, ϕ, θ or ν, are predetermined. The dispersion parameter vector $\boldsymbol{\varphi}_k^i$ is calculated to be

$$\boldsymbol{\varphi}_k^i = \boldsymbol{\varphi}_{k-1}^i + \mathbf{\Delta}_k^i. \tag{10}$$

The complex gain α_k^i is calculated analytically as

$$\alpha_k^i = \frac{(\boldsymbol{s}_k^i)^{\mathrm{H}}\boldsymbol{y}_k}{\|\boldsymbol{s}_k^i\|^2}, \tag{11}$$

where $(\cdot)^{\mathrm{H}}$ represents the Hermitian transpose, $\|\cdot\|$ denotes the Euclidian norm of the given argument, and the vector $\boldsymbol{s}_k^i$

contains the components

$$s^i(t; \boldsymbol{\varphi}_k^i) = \exp(j2\pi\nu_k^i t)c_m(\phi_k^i, \theta_k^i)u(t - \tau_k^i),$$
$$t \in [t_{k,m}, t_{k,m} + T_s), \ m = 1, \ldots, M.$$

The importance weights of the particles are calculated as

$$w_k^i = \frac{w_{k-1}^i p(\boldsymbol{y}_k|\mathbf{\Omega}_k^i)}{\sum\limits_{i=1}^{I} w_{k-1}^i p(\boldsymbol{y}_k|\mathbf{\Omega}_k^i)}, \quad i = 1, \ldots, I \tag{12}$$

with

$$p(\boldsymbol{y}_k|\mathbf{\Omega}_k^i) \propto \exp(-\frac{1}{2\sigma_n^2}\|\boldsymbol{y}_k - \alpha_k^i \boldsymbol{s}_k^i\|^2). \tag{13}$$

Step 2: Additional resampling. In a radar system which makes use of a multi-element Rx array and wideband transmission, e.g. of DVB-T signals, the number of temporal-spatial samples available in one measurement cycle is usually large. As a consequence, a significant mass of the posterior pdf $p(\mathbf{\Omega}_{1:k}|\boldsymbol{y}_{1:k})$ is concentrated around its modes. As the path parameters evolve over time, the particles that are distributed in **Step 1** can be too diffuse to "catch" the posterior probability mass. One brute-force solution is to employ a large number of particles. However the resulting complexity prohibits any practical implementation. This problem can be overcome with low complexity by using the local-likelihood-sampling method [14] and the local-importance-sampling method [15], both of which introducing window functions in the computation of the particle weights. It can also be solved by distributing the particles uniformly within a subset of the parameter space or using multi-hypothesis [16], [17]. However, all these methods have the drawback that the weighted particles do not approximate the true posterior density $p(\mathbf{\Omega}_{1:k}|\boldsymbol{y}_{1:k})$, and consequently the estimation results can be artifacts.

In this contribution, we introduce an additional resampling step in which two techniques are used for allocation of particles without misinterpreting the posterior density. This step is activated when the importance weights of the particles obtained from (12) are all negligible. The first technique consists in dropping some components in $\boldsymbol{y}_k$ when calculating the importance weights. We denote the remained components of $\boldsymbol{y}_k$ by $\tilde{\boldsymbol{y}}_k$. As the number of components in $\tilde{\boldsymbol{y}}_k$ is less than that in $\boldsymbol{y}_k$, the posterior pdf $p(\mathbf{\Omega}_k|\tilde{\boldsymbol{y}}_k, \boldsymbol{y}_{1:k-1})$ is less concentrated than the original pdf $p(\mathbf{\Omega}_k|\boldsymbol{y}_{1:k})$. Thus, the particles have higher probability to get significant importance weights.

The second method consists in computing the importance weights as

$$\tilde{w}_k^i = \log p(\boldsymbol{y}_k|\mathbf{\Omega}_k^i) + \log w_{k-1}^i. \tag{14}$$

The obtained set $\{\mathbf{\Omega}_k^i, \tilde{w}_k^i\}$ is an estimate of the function $\log p(\mathbf{\Omega}_{1:k}|\boldsymbol{y}_{1:k})$. This function exhibits the same modes as $p(\mathbf{\Omega}_{1:k}|\boldsymbol{y}_{1:k})$ but it has a wider curvature in the vicinities of the modes. So, the probability to get non-negligible importance weights is enhanced.

Based on these two methods, we propose an additional resampling step which can be implemented with the following pseudo-code.

for $n = 1$ to N **do**

Step 2.1 Select vector $\tilde{\boldsymbol{y}}_k^n$ which contains some of the components of $\boldsymbol{y}_k$. The number of components in $\tilde{\boldsymbol{y}}_k^n$ should increase with respect to n.

Step 2.2 Calculate the importance weights $\tilde{w}_k^i$, $i = 1, \ldots, I$ according to (14) with $\boldsymbol{y}_k$ replaced by $\tilde{\boldsymbol{y}}_k^n$.

if $\{\tilde{w}_k^i\}$ contains non-significant values, e.g. less than $\max\{\tilde{w}_k^i\} - 3$, **then**

    Step 2.3 Find the indices $\boldsymbol{A} = \{i^{\text{s}}\}$ of the particles with significant importance weights. Let D denote the number of particles with non-significant weights.

    Step 2.4 Generate D new particles with states drawn from $p(\boldsymbol{\Omega}_k | \boldsymbol{\Omega}_{k-1}^{j(\boldsymbol{A}_d)})$, $d = 1, \ldots, D$. Here, $\boldsymbol{A}_d$ denotes the dth element of $\boldsymbol{A}$, and $j(\boldsymbol{A}_d)$ is the index of a particle in the $(k-1)$th observation from which the $\boldsymbol{A}_d$th particle in the kth observation is generated. Replace the particles that have non-significant weights by the new particles.

    Step 2.5 Update the importance weights w_{k-1}^i as

$$w_{k-1}^i = J(i)^{-1} w_{k-1}^{j(i)}, \quad i = 1, \ldots, I, \qquad (15)$$

    where $J(i)$ represents the total number of new particles generated using the $j(i)$th particle in the $(k-1)$th observation. Go to **Step 2.2**.

    end if

  end for

Step 3: Standard resampling. The operations performed in this step are similar to those shown in the loop in **Step 2** except that the importance weights $\tilde{w}_k^i$ are replaced by w_k^i and the observation $\tilde{\boldsymbol{y}}_k^n$ is substituted with $\boldsymbol{y}_k$.

Step 4: Estimate the posterior pdf. The estimate of the posterior pdf can be approximated based on the particles and their importance weights according to

$$\hat{p}(\boldsymbol{\Omega}_{1:k} | \boldsymbol{y}_{1:k}) = \sum_{i=1}^{I} w_k^i \delta(\boldsymbol{\Omega}_{1:k} - \boldsymbol{\Omega}_{1:k}^i). \qquad (16)$$

This pdf estimate can be used to estimate the expectation of a function of $\boldsymbol{\Omega}_{1:k}$. For example, the state vector $\boldsymbol{\Omega}_{1:k}$ can be estimated as

$$\hat{\boldsymbol{\Omega}}_{1:k} = \sum_{i=1}^{I} \boldsymbol{\Omega}_{1:k}^i w_k^i. \qquad (17)$$

C. Extension to Multi-Target Scenarios

The proposed PF can be multiplicated to cope with a multiple-target scenario in the case where the parameters of any two different target signals are always distinct. Notice that this situation is frequently encountered in reality. For instance, even though two targets are close to each other in space, they are likely to differ in velocity and therefore the signals reflected by them differ in Doppler frequency. In this case each PF tracks the parameters of the signal of one specific target. Its particle states are initialized using the parameter estimates of the signal contributed by the corresponding target. The Space-Alternating Generalized Expectation-Maximization (SAGE) algorithm [18] can be used to compute approximates of the ML estimates of these parameters with low complexity.
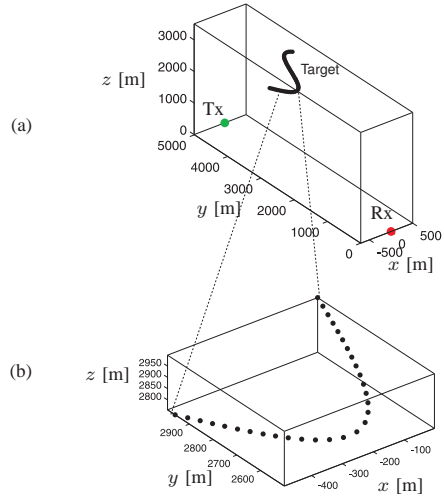
Fig. 2. Synthetic trajectories of an air-borne target.

IV. SIMULATION STUDIES

Simulation studies are conducted to evaluate the performance of the proposed PF in a single-target scenario. We consider a bistatic radar system with one Tx broadcasting a DVB-T signal defined in [19] as "illuminator of opportunity" and one Rx. The locations of the Tx and Rx are known in advance. The Rx is equipped with a 6×6 planar array with isotropic antennas. The orientation of the array, i.e. the direction with $\phi = 0°$ and $\theta = 0°$, points towards the Tx location. The Rx is equipped with a switch that operates in the TDM mode depicted in Fig. 1. Table I shows the specification of the DVB-T signal and the timing of the data acquisition considered in the simulations. The sensing period T_s is set equal to the duration of one DVB-T orthogonal frequency division multiplexing (OFDM) symbol.

Table II reports the intrinsic resolution ability and the estimation range of the considered bistatic radar system. The resolutions in azimuth and elevation of arrival are computed according to [18, Eq. 31]. The resolution in Doppler frequency equals $1/[(M-1)T_r + T_s]$ [20]. The delay estimation range reported in Table II is relative to the delay of the reference signal.

In the considered synthetic environment, an air-borne target flies with a constant speed of 500 km/h along a trajectory between the Tx and Rx locations, which are fixed. Fig. 2 (a) depicts the Tx and Rx locations, and the target trajectory in a 3-dimensional Cartesian coordinate system. Fig. 2 (b) illustrates the "zoomed-in" image of a fragment of the target trajectory.

TABLE I

PARAMETERS OF THE DVB-T SIGNAL AND DATA ACQUISITION TIMING CONSIDERED IN THE SIMULATIONS

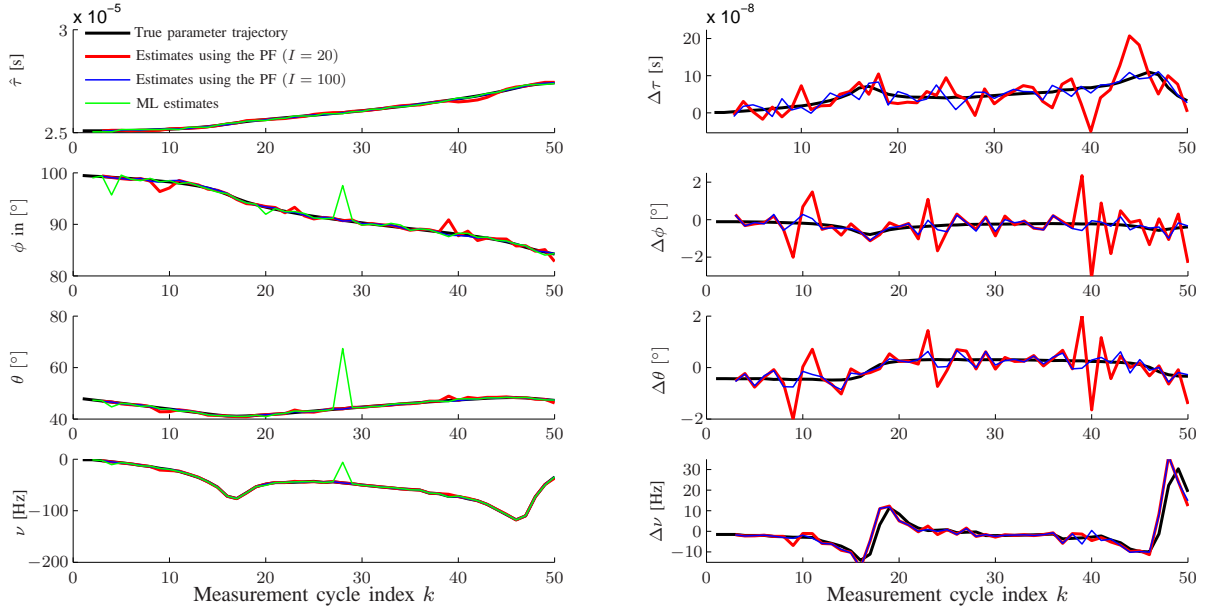| Item	Value
DVB-T mode [19]	2K
Center carrier frequency	300 MHz
Sensing period T_s	0.28 ms
Switching period T_r	$2 \cdot T_s$
Cycle interval T_{cy}	$1000 \cdot T_s$

Fig. 3. True parameter trajectories and their estimates obtained using the PF and the ML method.

In this synthetic environment the DVB-T signal broadcast by the Tx is reflected by the target before it is received at the Rx. The parameters characterizing the target signal can be related to the locations of the Tx and the Rx, and the target trajectory. The delay of the target signal at the kth measurement cycle τ_k reads

$$\tau_k = (\|\boldsymbol{r}_{\mathrm{tg},k} - \boldsymbol{r}_{\mathrm{Tx}}\| + \|\boldsymbol{r}_{\mathrm{tg},k} - \boldsymbol{r}_{\mathrm{Rx}}\|)/c, \qquad (18)$$

where $\boldsymbol{r}_{\mathrm{Tx}}$ and $\boldsymbol{r}_{\mathrm{Rx}}$ denote the location vector of the Tx and the Rx respectively, $\boldsymbol{r}_{\mathrm{tg},k}$ is the target location vector at the beginning of the kth measurement cycle, and c denotes the speed of light. The elevation and azimuth of arrival of the signal are computed to be respectively

$$\theta_k = \cos^{-1}(\omega_{k,z}) \qquad (19)$$

$$\phi_k = \cos^{-1}(\omega_{k,x}/\sqrt{\omega_{k,x}^2 + \omega_{k,y}^2}), \qquad (20)$$

where $\omega_{k,x}$, $\omega_{k,y}$, $\omega_{k,z}$ are the entries of the vector

$$\boldsymbol{\omega}_k = \frac{\boldsymbol{r}_{\mathrm{tg},k} - \boldsymbol{r}_{\mathrm{Rx}}}{\|\boldsymbol{r}_{\mathrm{tg},k} - \boldsymbol{r}_{\mathrm{Tx}}\|}. \qquad (21)$$

The Doppler frequency is approximated as

$$\nu_k \approx \lambda^{-1} T_{cy}^{-1}(\tau_k - \tau_{k-1}) \cdot c, \qquad (22)$$

where λ is the wavelength. The rate of change parameters $\Delta(\cdot)_k$ are computed to be

$$\Delta(\cdot)_k = T_s^{-1}[(\cdot)_k - (\cdot)_{k-1}] \qquad (23)$$

TABLE II

INTRINSIC RESOLUTION ABILITY AND ESTIMATION RANGES OF THE USED

PASSIVE RADAR SYSTEM.

Dimension	Intrinsic resolution	Estimation range
Azimuth	$\approx 19.1°$	$[0°, 180°)$
Elevation	$\approx 19.1°$	$[0°, 180°)$
Delay	$0.109\ \mu s$	$[0, 280]\ \mu s$
Range	32.8 m	$[0, 84]$ km
Doppler frequency	50 Hz	$[-457, 457]$ kHz

with $(\cdot)$ being replaced by τ, ϕ, θ or ν. The black solid curves shown in Fig. 3 depict an example of time evolution of the true values of these parameters generated with the linear state-space model (6) over an interval corresponding to 50 measurement cycles. For simplicity, $\alpha_1 = \exp(j\pi/4)$ is used and the driving processes $w_{|\alpha|,k}$ and $w_{\arg(\alpha),k}$, $k = 1, \dots, K$ with K representing the total number of considered measurement cycles are set to zeros. The samples $\boldsymbol{y}_k$, $k = 1, \dots, K$ of the received signal are generated using the observation model (1). The signal-to-noise ratio (SNR) is set to -10 dB, which complies with the measurement results reported in [21].

The parameter estimates obtained by applying the proposed PF to the sequence of these samples are also depicted in Fig. 3. The estimates of the dispersion parameters obtained by applying the sample-based ML method to the signals received in individual cycles are shown as well. It can be observed that the PF is capable of tracking the signal parameters over the whole considered observation interval. The ML estimator exhibits significant estimation error in measurement cycle 28, resulting in a "loss-of-track" error. Additional simulation results not reported here demonstrate that the PF does not exhibit "loss-of-track" errors provided the number I of particles is larger than 20. From Fig. 3, we also observe that the RMSEEs are decreasing as I increases. This behaviour is more evident in tracking the rates of change parameters (see the figures in the right column of Fig. 3).

The root-mean-square-estimation-errors (RMSEEs) obtained using the PFs with $I = 20, 40, \dots, 200$ are depicted in Fig. 4. It is observed that the RMSEEs decrease as the number I of particles increases and stabilize for $I \geq 50$. Simulation results not shown here also demonstrate that with $I \geq 40$ the PF returns RMSEEs lower than those obtained with the sample-based ML estimator for all considered parameters.

It is worth mentioning that the comparison between the proposed PF and the sample-based ML parameter estimator is not fair, since the latter estimator does not exploit the
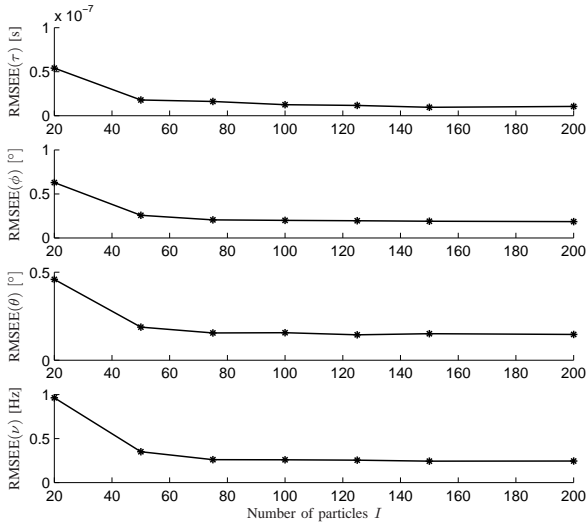
other in space, they are likely to differ in velocity and therefore the signals reflected by them differ in Doppler frequency.

Fig. 4. RMSEEs of the PF versus the number I of used particles.

knowledge that the signal parameters are generated using a linear state-space model. However, this comparison evidences that by taking into account the time-evolution behaviour of the parameters, algorithms, e.g. the PF proposed here, yield higher estimation accuracy and robustness compared to conventional algorithms that do not exploit this dynamics. Another benefit of using the proposed PF is that, the problem of association of the parameter estimates computed from the individual signal samples is inherently solved. Therefore, the association step required in some of the conventional tracking algorithms, e.g. [1], [4], is unnecessary.

V. CONCLUSIONS

In this contribution, we developed a particle filter (PF) for tracking of the multi-dimensional parameters of the received signal contributed by a moving target. The tracked parameters are the delay (time of arrival), the azimuth and elevation of arrival, the Doppler frequency, the complex amplitude of the target signal, as well as the rates of change of all but the last parameter. The dynamics of these parameters is described using a linear state-space model. The proposed PF accurately estimates the posterior probability density function (pdf) of these parameters from observations of the target signal with a small number of particles. A modified step that accounts for the high concentration of the posterior probability distribution of the parameters makes this possible.

We implemented the PF in a bistatic radar system that uses digital-video-broadcast terrestrial (DVB-T) transmission as "illuminator of opportunity". Simulation results show that the proposed PF is able to track the parameters of a target signal with a small number of particles, resulting in a low computational complexity. The PF returns lower estimation errors and is more robust than the maximum likelihood estimator applied to individual signal samples.

The proposed PF can be used to track the parameters of the individual signals contributed by multiple targets when the states of signal parameter vectors for different targets are distinct. Notice that this situation is frequently encountered in reality. For instance, even though two targets are close to each

REFERENCES

[1] P. Howland, "Target tracking using television-based bistatic radar," *IEE Proceedings - Radar, Sonar and Navigation*, vol. 146, pp. 166–174, 1999.
[2] S. Herman and P. Moulin, "A particle filtering approach to FM-band passive radar tracking and automatic target recognition," in *Proceedings of IEEE Aerospace Conference*, vol. 4, 2002, pp. 1789–1808.
[3] C. Hue, J.-P. L. Cadre, and P. Perez, "Tracking multiple objects with particle filtering," *IEEE Transactions on Aerospace and Electronic Systems*, vol. 38, no. 3, pp. 791–812, Jul 2002.
[4] P. Howland, D. Maksimiuk, and G. Reitsma, "FM radio based bistatic radar," *IEE Proceedings - Radar, Sonar and Navigation*, vol. 152, no. 3, pp. 107–115, 2005.
[5] Y. Boers, H. Driessen, J. Torstensson, M. Trieb, R. Karlsson, and F. Gustafsson, "Track-before-detect algorithm for tracking extended targets," *IEE Proceedings - Radar, Sonar and Navigation*, vol. 153, no. 4, pp. 345–351, 2006.
[6] M. Rutten, N. Gordon, and S. Maskell, "Recursive track-before-detect with target amplitude fluctuations," *IEE Proceedings - Radar, Sonar and Navigation*, vol. 152, no. 5, pp. 345–352, 2005.
[7] Y. Boers and D. Salmond, "Editorial: Target tracking: algorithms and applications," *IEE Proceedings - Radar, Sonar and Navigation*, vol. 152, no. 5, pp. 289–290, 2005.
[8] Y. Boers and J. Driessen, "Multitarget particle filter track before detect application," *Radar, Sonar and Navigation, IEE Proceedings -*, vol. 151, no. 6, pp. 351–357, 10 Dec. 2004.
[9] M. I. Skolnik, *Radar handbook*, 2nd ed. McGraw-Hill Professional, 1990, ISBN 007057913X.
[10] J. Baniak, G. Baker, A. Cummingham, and L. Martin, "Silent sentry passive surveillance," in *Proceedings of Aviation Week and Space Technology*, July 1999.
[11] S. Herman, "A particle filtering approach to joint passive radar tracking and target classification," Ph.D. dissertation, University of Illinois, 2002.
[12] B. H. Fleury, X. Yin, P. Jourdan, and A. Stucki, "High-resolution channel parameter estimation for communication systems equipped with antenna arrays," in *Proceedings of the 13th IFAC Symposium on System Identification (SYSID)*, no. ISC-379, Rotterdam, The Netherlands, 2003.
[13] X. Yin, T. Pedersen, N. Czink, and B. H. Fleury, "Parametric characterization and estimation of bi-azimuth and delay dispersion of path components," in *Proceedings of The First European Conference on Antennas and Progation (EuCAP'06)*, Acropolis, Nice, France, November 2006.
[14] P. Torma and C. Szepesvári, "Enhancing particle filters using local likelihood sampling," in *Proceedings of the 8th European Conference on Computer Vision (ECCV)*, 2004.
[15] ——, "Local importance sampling: A novel technique to enhance particle filtering," *Journal of Multimedia*, vol. 1, no. 1, pp. 32–43, April 2006.
[16] D. Fox, W. Burgard, F. Dellart, and S. Thrun, "Monte Carlo localization: Efficient position estimation for mobile robots," in *Proceedings of the 16th National Conference on Artificial Intelligence*, Orlando, FL, USA, 1999.
[17] S. Lenser and M. Veloso, "Sensor resetting localization for poorly modelled mobile robots," in *Proceedings of IEEE International Conference on Robotics and Automation (ICRA'00)*, vol. 2, 2000, pp. 1225–1232.
[18] B. H. Fleury, M. Tschudin, R. Heddergott, D. Dahlhaus, and K. L. Pedersen, "Channel parameter estimation in mobile radio environments using the SAGE algorithm," *IEEE Journal on Selected Areas in Communications*, vol. 17, no. 3, pp. 434–450, Mar. 1999.
[19] ETSI, *ETSI EN 300 744 v1.5.1: Digital Video Broadcasting (DVB); Framing structure, channel coding and modulation for digital terrestrial television*, European Broadcasting Union, Nov. 2004. [Online]. Available: http://www.etsi.org
[20] T. Pedersen, C. Pedersen, X. Yin, B. H. Fleury, R. R. Pedersen, B. Bozinovska, A. Hviid, P. Jourdan, and A. Stucki, "Joint estimation of Doppler frequency and directions in channel sounding using switched Tx and Rx arrays," in *Proceedings of IEEE Global Telecommunications Conference (Globecom)*, vol. 4, December 2004, pp. 2354–2360.
[21] R. Pollard, "How passive radar sensors can support air traffic control," BAE Systems, Advanced Technology Centre, Tech. Rep., 2006.